Application of a Control-Volume-Based Finite-Element Formulation to the Shock Tube Problem

S. M. H. Karimian* and G. E. Schneider†
University of Waterloo,
Waterloo, Ontario N2L 3G1, Canada

Introduction

IN this article, the performance of a newly developed pressure-based method for incompressible/compressible flow calculation is investigated by solving the shock tube problem. This problem has served as a benchmark case in the literature,[1,2] since it has many transient flow features. Pressure-based methods have been increasingly used for the solution of compressible flow.[3,4] The present method is a generalized version of the method of Ref. 5, which was developed for incompressible flow computation, using primitive variables.[5] Primitive-variable methods are widely used in the incompressible range. Here it is demonstrated that the present method is also very capable of solving transient and compressible flows incorporating strong discontinuities.

The governing equations are discretized using a control-volume-based finite element (CVBFE) method. The CVBFE method was initially developed for the solution of heat transfer and fluid flow problems.[6,7] Later, its application to compressible flow computation was presented in the literature.[8,9] With the use of a new formulation for the mass conserving velocity (or convecting velocity), proposed by Karimian and Schneider,[10] a strong coupling between pressure and velocity is created which does not allow any kind of checkerboard oscillations. The effect of three different methods for energy flux evaluation on the results are also examined in this article. The present results agree very well with the exact solution. No explicit artificial viscosity is added to the solution.

Numerical Method

The conservation form of the one-dimensional unsteady Euler equations are given by

$$\frac{\partial \boldsymbol{Q}}{\partial t} + \frac{\partial \boldsymbol{E}}{\partial x} = 0 \tag{1}$$

where $\boldsymbol{Q} = \{\rho, \rho u, \rho e\}^T$ is the conserved quantity vector, $e = c_v T + u^2/2$ is the total energy, $\rho = p/RT$ is density for a perfect gas, and the convection flux vector is

$$\boldsymbol{E} = \{\rho u, (\rho u)u + p, (\rho u)e + up\}^T \tag{2}$$

As is shown in Fig. 1, each element is divided into two subcontrol volumes (SCV). For each node, a control volume is formed that includes the two neighboring SCVs. In the CVBFE method a matrix elemental equation is formed by integrating Eq. (1) over each SCV within the element, e.g., SCV_i and SCV_{i+1} for the element $i + \frac{1}{2}$. This requires the transient term to be averaged over the SCVs and the convection flux vector to be evaluated at the common surface of the two SCVs within the element, e.g. surface $i + 1/2$ (note that element $i + 1/2$ will be the sample element in the rest of the article). The assembly procedure of the matrix elemental equations of all elements, then, will result in the formation of control-volume equations; for details see Ref. 11.

The transient term is modeled using backward difference in time and the average value of $\boldsymbol{Q}$ over the SCV is represented by its nodal value associated with that SCV, e.g. Q_i for SCV_i. The components ρ, ρu, and ρe in $\boldsymbol{Q}$ are linearized by the Newton method with respect to p and T, ρ and u, and ρ and e, respectively.[11]

In the convection flux vector $\boldsymbol{E}_{i+\frac{1}{2}}$, the pressure terms are modeled using bilinear interpolation. The convected quantities u and e that appear in the momentum and energy equations, respectively, will be modeled using the physical influence scheme (PIS) of Ref. 7; for a brief overview of other methods see Ref. 12. For the convecting velocity that appears in the mass flux and will be indicated by caret, i.e., $\hat{u}$, a different formulation is used. The treatment of density is somewhat similar to that of the convected quantities. Using the new notation, the convection flux vector at $i + 1/2$ is represented by

$$\boldsymbol{E}_{i+\frac{1}{2}} = \{\rho\hat{u}, (\rho\hat{u})u + p, (\rho\hat{u})e + \hat{u}p\}^T_{i+\frac{1}{2}} \tag{3}$$

The underlying principle of PIS is to bring the correct physical influence of the problem into the convected quantity formulation. This is done by algebraically approximating the relevant governing equation for the quantity in question at the control-volume surface. For the fluid flow prediction, the nonconservative form of the momentum equation given by

$$\rho\frac{\partial u}{\partial t} + \rho u\frac{\partial u}{\partial x} + \frac{\partial p}{\partial x} = 0 \tag{4}$$

can be considered as the transport equation for the convected velocity. Each term of this equation is modeled at $i + \frac{1}{2}$, based on the physics of the problem. Assuming that the flow is going from left to right, after modeling and rearrangement the following expression for the convected velocity is obtained:

$$u_{i+\frac{1}{2}} = U_i + \left\{\frac{P_i - P_{i+1}}{2\overline{\rho u}[1 + (1/2C)]}\right\} + \left[\frac{u^o_{i+\frac{1}{2}} - \bar{U}_i}{(1 + 2C)}\right] \tag{5}$$

where the Courant number is $C = \bar{u}(\Delta t/\Delta x)$. The overbar and superscript o denote the lagged values from the previous iteration and the previous time step, respectively, and the variables U and P denote nodal values of velocity and pressure, respectively. There are three forms of the energy equation that can be modeled at $i+\frac{1}{2}$, to obtain a formulation for the convected total energy at this point. In the following, these energy equations and the corresponding formulations for $e_{i+\frac{1}{2}}$, which are obtained after modeling and rearrangement of the relevant energy equation, are presented.

The first choice is the nonconservative form of the energy equation given by

$$\rho\frac{\partial e}{\partial t} + \rho u\frac{\partial e}{\partial x} + \frac{\partial (up)}{\partial x} = 0 \tag{6}$$

from which $e_{i+\frac{1}{2}}$ is obtained as

$$e_{i+\frac{1}{2}} = \frac{\left(c_v T_i + \frac{1}{2}\bar{U}_i U_i\right) + \{[(\bar{P}U)_i - (\bar{P}U)_{i+1}]/2\overline{\rho u}\}}{[1 + (1/2C)]} + \frac{e^o_{i+\frac{1}{2}}}{(1 + 2C)} \tag{7}$$

The second one is the thermal energy equation given by

$$\rho c_v\frac{\partial T}{\partial t} + \rho u c_v\frac{\partial T}{\partial x} + p\frac{\partial u}{\partial x} = 0 \tag{8}$$

which depicts the transport nature of temperature. From this equation $T_{i+\frac{1}{2}}$ is obtained as

$$T_{i+\frac{1}{2}} = \frac{T_i + \bar{p}_{i+\frac{1}{2}}[(U_i - U_{i+1})/2\overline{\rho u}c_v]}{[1 + (1/2C)]} + \frac{T^o_{i+\frac{1}{2}}}{(1 + 2C)} \tag{9}$$

which is substituted in $[c_v T + (\tilde{u}^2/2)]_{i+\frac{1}{2}}$ to represent $e_{i+\frac{1}{2}}$. The $\tilde{u}$ would be the average of two nodal velocities $\bar{U}_i$ and $\bar{U}_{i+1}$.

The third option is to choose the following form of the energy equation:

$$\rho\frac{\partial h}{\partial t} - \frac{\partial p}{\partial t} + \rho u\frac{\partial h}{\partial x} = 0 \tag{10}$$

Received Nov. 8, 1993; presented as Paper 94-0131 at the AIAA 32nd Aerospace Sciences Meeting, Reno, NV, Jan. 10–13, 1994; revision received July 29, 1994; accepted for publication July 29, 1994.

*Research Assistant, Department of Mechanical Engineering. Member AIAA.

†Professor, Department of Mechanical Engineering. Member AIAA.

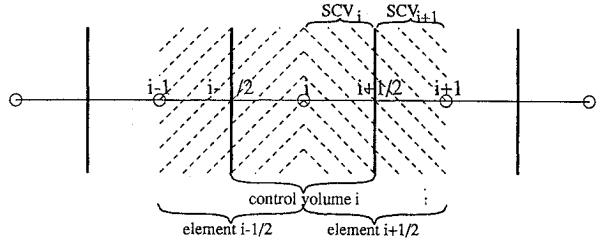

Fig. 1 One-dimensional grid structure.

and find the value of total enthalpy as

$$h_{i+\frac{1}{2}} = \frac{\left(c_p T_i + \frac{1}{2}\bar{U}_i U_i\right)}{[1+(1/2C)]} + \frac{h^o_{i+\frac{1}{2}} + \left[\left(p_{i+\frac{1}{2}} - p^o_{i+\frac{1}{2}}\right)/\bar{\rho}\right]}{(1+2C)} \tag{11}$$

in which h_i has been substituted for by $c_p T_i + \frac{1}{2}\bar{U}_i U_i$. Equation (11), then, will be used to represent the term $(e + p/\rho)$ in Eq. (3).

The mass flux $\rho\hat{u}$ in the second and third components of Eq. (3) is evaluated using lagged values from the previous iteration. However, the mass flux in the continuity equation, i.e., the first component of Eq. (3), is linearized with respect to both density and velocity, i.e.,

$$\rho\hat{u} \approx \bar{\rho}\hat{u} + \rho\bar{u} - \bar{\rho}\bar{u} \tag{12}$$

where $\bar{u} = \bar{\hat{u}}$ (this is also true for the previous equations). In this case as the effect of compressibility becomes more important, particularly in supersonic flow, the hyperbolic behavior of pressure through ρ, in the term $\rho\bar{u}$, becomes dominant. This is enforced by implementing the following formulation for the density:

$$\rho_{i+\frac{1}{2}} = \frac{1}{R\bar{T}_i} P_i + (\Delta\rho) \tag{13}$$

where $\Delta\rho$ is the density correction term that will be introduced shortly. The convecting velocity formulation is given by

$$\hat{u}_{i+\frac{1}{2}} = \frac{U_i + U_{i+1}}{2} + \frac{P_i - P_{i+1}}{2\overline{\rho u}[1+(1/2C)]} + \text{TERMS} \tag{14}$$

where

$$\text{TERMS} = \frac{\bar{u}^2(\bar{\rho}_{i+1} - \bar{\rho}_i) + (\bar{u}^2/C)\left(\bar{\rho}_{i+\frac{1}{2}} - \rho^o_{i+\frac{1}{2}}\right)}{2\overline{\rho u}[1+(1/2C)]} + \frac{u^o_{i+\frac{1}{2}} - \tilde{u}_{i+\frac{1}{2}}}{(1+2C)} \tag{15}$$

TERMS contains the part of formulation that is due to compressibility and transition in time and is evaluated using lagged values from the previous iteration. As was mentioned, the present formulation is the extension of an originally developed numerical method for the incompressible flow calculation, in which Eq. (14), with TERMS = 0, was proposed to surmount the checkerboard oscillations. With the above formulations two values of velocity have been used at $i + \frac{1}{2}$; one is the convected velocity given by Eq. (5), and the other is the convecting velocity given by Eq. (14). These two velocities will become very close to each other in the converged solution. Implementation of two such velocities at the control-volume surface has been found essential to suppress pressure oscillations.[5,8,13] More details about the derivation of Eq. (14) can be found in Refs. 5, 10, and 11.

Very similar to the evaluation of the convected quantities, at high-speed supersonic flow $\Delta\rho$ can be evaluated by modeling and rearrangement of the continuity equation at $i + \frac{1}{2}$. However, in the incompressible limit, where the density is nearly constant, $\Delta\rho$ is approximated by $(\bar{\rho}_{i+1} - \bar{\rho}_i)/2$. In this study our experience indicates that for the shock tube problem, both methods result in the very same numerical solutions. Therefore, to reduce the computational effort $\Delta\rho$ is calculated from $(\bar{\rho}_{i+1} - \bar{\rho}_i)/2$.

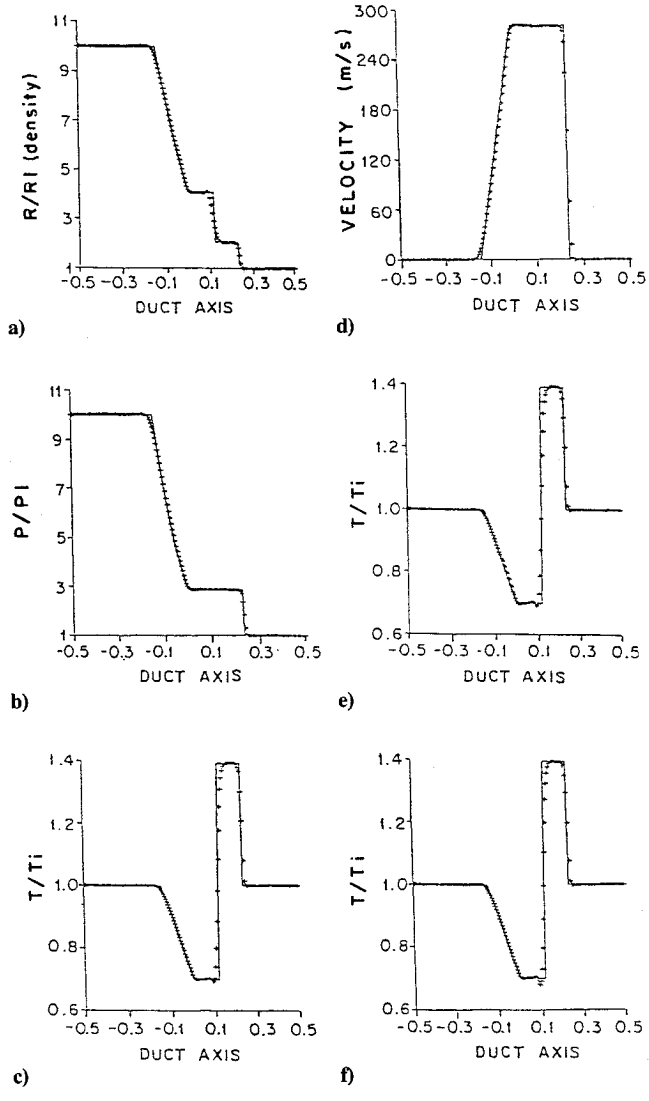

Fig. 2 Results of the shock tube problem with 200 nodes at t = 0.42 ms, energy flux calculated: a–d) using Eq. (9), e) using Eq. (7), and f) Using Eq. (11).

The formulation of the method is now complete. However, a few comments need to be made. First, the method is second-order accurate in space. Second, the method is fully implicit and, therefore, first order in time. Third, to avoid the under/overshoots in the vicinity of the moving shock and contact discontinuity in the numerical solution, the values of $\Delta\rho$ in Eq. (13) and TERMS in Eq. (14) are not calculated directly, but using an absolute harmonic interpolation in the entire domain; for details see Ref. 11.

Numerical Results

The flow is initially at rest in a 1 m long duct, which is equally divided by a diaphragm into a high-pressure region (1013.0 kPa) and a low-pressure (101.3 kPa) region. At $t = 0$, temperature is 293 °K in both regions. Other gas properties are c_v = 717.0 J/kg °K, R = 286.0 J/kg °K and γ = 1.40. A uniform grid with 200 nodes is used, and the solution was stopped at t = 0.42 ms with a time step of $\Delta t = 4.0 \times 10^{-6}$ s. The pressure, density, and temperature distributions are nondimensionalized by the initial pressure and density at the low-pressure region and the initial temperature, respectively. At each time step the solution is converged to meet the following criterion:

$$\text{Max}\left(\left|\frac{P_i - \bar{P}_i}{P_i}\right|, \left|\frac{T_i - \bar{T}_i}{T_i}\right|\right) < \epsilon$$

where $i = 1, \ldots, N$ with N being the total number of nodes and ϵ = 0.01. Numerical results of the present method, using Eq. (9)

to evaluate energy flux at the control-volume surface, are in very good agreement with the exact solution in Figs. 2a–2d. The moving shock wave is captured very sharply within a few nodes. The pressure and velocity solutions are almost exact, however, there is a minor undershoot before the contact discontinuity in the temperature distribution. Since the density is calculated from the equation of state, its value is completely dependent on the pressure and temperature fields. The effect of using Eqs. (7) and (11) to evaluate the energy flux at the control-volume surface is shown in Figs. 2e and 2f, respectively. The pressure and velocity distributions are not shown here; they are similar to the results in Figs. 2b and 2d, except that for the velocity distributions there exists a small overshoot at $x = 0.0$. A temperature undershoot higher than that in Figs. 2c and 2e is seen in Fig. 2f. However, there is not much difference in the rest of the temperature distributions; see Ref. 11 for complete results.

In conclusion, for the numerical results, the overall accuracy of the method is found to be quite satisfactory, and no particular problem has been detected. All three forms of the energy flux evaluation can be used in this method, however, smoother results are obtained when Eq. (9) is used.

Acknowledgments

The financial support of the Natural Sciences and Engineering Research Council of Canada is gratefully acknowledged. The first author would like to thank the Ministry of Culture and Higher Education of Iran for the scholarship he received.

References

[1]Montagne, J. L., Yee, C., and Vinokur, M., "Comparative Study of High Resolution Shock Capturing Schemes for Real Gas," *AIAA Journal*, Vol. 27, No. 10, 1989, pp. 1332–1346.

[2]Lin, H., and Chieng, C. C., "Characteristic-Based Flux Limiters of an Essentially Third-Order Flux Splitting Method for Hyperbolic Conservation Laws," *International Journal for Numerical Methods in Fluids*, Vol. 13, No. 3, 1991, pp. 287–307.

[3]Karki, K. C., and Patankar, S. V., "Pressure-Based Calculation Procedure for Viscous Flows at All Speeds in Arbitrary Configurations," *AIAA Journal*, Vol. 27, No. 9, 1989, pp. 1167–1174.

[4]Shyy, W., Chen, M. H., and Sun, C. S., "Pressure-Based Multigrid Algorithm for Flow at All Speeds," *AIAA Journal*, Vol. 30, No. 11, 1992, pp. 2660–2669.

[5]Schneider, G. E., and Karimian, S. M. H., "Advances in Control-Volume Based Finite-Element Methods for Compressible Flows," *Computational Mechanics*, Vol. 14, No. 5, 1994, pp. 431–446.

[6]Baliga, B. R., and Patankar, S. V., "A Control Volume Finite-Element Method for Two-Dimensional Fluid Flow and Heat Transfer," *Numerical Heat Transfer*, Vol. 6, No. 3, 1983, pp. 245–261.

[7]Schneider, G. E., and Raw, M. J., "Control-Volume Finite-Element Method for Heat Transfer and Fluid Flow Using Co-located Variables —1. Computational Procedure," *Numerical Heat Transfer*, Vol. 11, No. 4, 1987, pp. 363–390.

[8]Raw, M. J., Galpin, P. F., and Raithby, G. D., "The Development of an Efficient Turbomachinery CFD Analysis Procedure," AIAA Paper 89-2394, 1989.

[9]Naterer, G. F., and Schneider, G. E., "Use of the Second Law in a Predictive Capacity for Compressible Fluid Flow Discrete Analysis," AIAA, Washington, DC, 1992 (AIAA Paper 92-2942).

[10]Karimian, S. M. H., and Schneider, G. E., "Pressure-Based Computational Method for Compressible and Incompressible Flows," *Journal of Thermophysics and Heat Transfer*, Vol. 8, No. 2, 1994, pp. 267–274.

[11]Karimian, S. M. H., and Schneider, G. E., "Application of a New Control-Volume-Based Finite-Element Formulation to the Shock Tube Problem," AIAA Paper 94-0131, 1994.

[12]Van Doormaal, J. P., Turan, A., and Raithby, G. D., "Evaluation of New Techniques for the Calculation of Internal Recirculating Flows," AIAA Paper 87-0059, 1987.

[13]Rhie, C. M., and Chow, W. L., "Numerical Study of the Turbulent Flow Past an Airfoil with Trailing Edge Separation," *AIAA Journal*, Vol. 21, No. 11, 1983, pp. 1525–1532.

Simulating Heat Addition via Mass Addition in Constant Area Compressible Flows

W. H. Heiser,* W. B. McClure,† and C. W. Wood†
U.S. Air Force Academy, Colorado 80840

Introduction

THE one-dimensional flow analyses of this study demonstrate the interesting and potentially useful similarities between the influence of heat addition and of mass addition (injected normal to the flow at the same total temperature) on compressible duct flows.

For the most part, the effect of a given fractional mass flow addition on flow properties is equivalent to twice that amount of fractional total temperature increase. This conclusion applies in particular to the important phenomena of choking and wall boundary-layer separation, the latter resulting from the adverse pressure gradients created by heat or mass addition in supersonic flows. Wall boundary-layer separation is, in fact, so natural to such flows that it appears to often precede any choking that would otherwise occur.

The results of this study suggest that some aspects of the complex behavior of dual-mode ramjet/scramjet combustors[1] could be experimentally evaluated or demonstrated by replacing combustion with less expensive, more easily controlled, safer mass addition.

The first clue to the strength of the analogy is revealed by the well-known influence coefficients of one-dimensional compressible flows (e.g., Table 8.2 of Ref. 2), several of the most important of which are found in Table 1. The clear message of this tabulation is that the incremental influence of a given fractional change of mass flow rate $\delta\dot{m}/\dot{m}$ on Mach number M, static pressure p, and total pressure p_t is exactly double that of an equal fractional change of total temperature $\delta T_t/T_t$ for the same ratio of specific heats γ.

Simple Mass or Heat Addition Flows

The analyses that follow next are based on the classical one-dimensional model of the steady, constant throughflow area flow of a calorically perfect gas.[2] In addition to the traditional model, it will be assumed that any mass addition has the same total temperature and imposition as the inlet flow and is injected normal to the duct axis (i.e., without contributing to the axial momentum) and, unless otherwise noted, the flow is frictionless.

The reader will recognize that many of these assumptions are made for convenience, rather than out of necessity. Solutions to the governing equations could be obtained with less restrictive assumptions (e.g., the case of combined mass addition and wall friction that appears later) but at a price we believe to be disproportionate to the benefit, including the loss of simplicity and transparency. These assumptions have led to fruitful results throughout the history of compressible fluid mechanics, as they will for the situation at hand.

When the throughflow area is constant and only one forcing function (e.g., heat or mass addition) is present, these flows are commonly known as simple flows. They have many appealing and useful characteristics, the best known being that they yield closed-form algebraic solutions that depend on the single forcing function (e.g., Table 8.3 of Ref. 2). Simple flows have contributed generously to organizing our thinking, intuition, and experiences about compressible flows, and the present case will prove to be no exception. The simple flow involving heat addition is usually referred to as Rayleigh flow. The simple flow involving mass addition has no established designation, and will be referred to here as SMA flow.

The solution procedures for Rayleigh flow and SMA flow will not be reproduced in any detail here, but the same solutions can be

Received Oct. 18, 1993; revision received June 15, 1994; accepted for publication June 15, 1994.

*Professor, Department of Aeronautics. Fellow AIAA.
†Associate Professor, Department of Aeronautics. Senior Member AIAA.